Geological Quarterly, 2025, 69, 47
DOI: https://doi.org/10.7306/gq.1820

Active weathering processes: composition and geochemistry of secondary sulphates from the Johan Hell mine, Maramureş, Romania

Anna JANUSZEWSKA-KACPRZAK[1, 2, *], Rafał SIUDA[1] and Łukasz KRUSZEWSKI[3]

[1] University of Warsaw, Faculty of Geology, Żwirki i Wigury 93, 02-089 Warszawa, Poland; ORCID: 0000-0002-0444-2696 [A.J.-K.], 0000-0003-4153-8539 [R.S.]

[2] Polish Geological Institute – National Research Institute, Rakowiecka 4, 00-975 Warszawa, Poland

[3] Institute of Geological Sciences of the Polish Academy of Sciences, Twarda 51/55, 00-818 Warszawa, Poland; ORCID: 0000-0001-6332-9944 [Ł.K.]

Januszewska-Kacprzak, A., Siuda, R., Kruszewski, Ł., 2025. Active weathering processes: composition and geochemistry of secondary sulphates from the Johan Hell mine, Maramureş, Romania. Geological Quarterly, 69, 47; https://doi.org/10.7306/gq.1820

Associate Editor: Stanisław Zbigniew Mikulski

The Johan Hell mine, part of the Breiner polymetallic ore deposit in the Băiuţ mining area (Maramureş, Romania), hosts an exceptional diversity of secondary sulphate minerals formed through intense weathering of primary ore mineralization. This study provides a comprehensive mineralogical and geochemical characterization of efflorescent and crust-forming sulphates that developed under extreme acidic conditions. A total of 20 secondary minerals were identified, with halotrichite-group representatives being the most abundant and widespread, followed by römerite, voltaite, melanterite, rozenite, starkeyite, hexahydrite and szomolnokite. These minerals show strong compositional variability, influenced by local geochemical gradients and microenvironmental factors. Geochemical analyses (ICP-MS/ES) reveal significant enrichment of several elements – including Mn, Zn, Cu, As, REEs and Hg – particularly within the halotrichite group, voltaite and römerite. Mineral parageneses reflect a three-stage evolution of weathering conditions, controlled primarily by changes in pH and humidity. The progression from ultra-acidic (pH <2) to moderately acidic (pH 2.5–3.5) conditions governed the crystallization of the various hydrated sulphates.

Key words: secondary sulphates, voltaite, römerite, halotrichite group, toxic elements.

INTRODUCTION

The Băiuţ region (Fig. 1), situated ~40 km east of Baia Mare in Maramureş County, Romania, is characterized by significant polymetallic sulphide mineralization that has been intensively exploited since the 12th century. The most economically important elements were gold, silver, lead, zinc, copper and antimony. This area hosts a rich mining heritage and is recognized as one of Europe's most important metallogenic provinces. Mining operations continued until the early 21st century (Kovács et al., 2009). Previous research has primarily focused on the ore mineralization (Lang, 1979, 1994; Grancea et al., 2002; Costin, 2003, 2005; Damian et al., 2008, 2020; Plotinskaya et al., 2009), as well as on the environmental impact of prolonged mining activity, particularly soil and water contamination (Frentiu et al., 2008; Levei et al., 2009; Dorotan et al., 2018; Popa et al., 2019; Santanna et al., 2021).

In this region, three main ore deposits – Breiner, Văratec and Cisma – were exploited in several mines. The ore mineralization is subject to intense weathering processes in these areas. Variations in the composition of the primary mineralization and environmental conditions across the different mines result in distinct secondary mineral assemblages (for example, the Breiner mine; Januszewska et al., 2025).

During the decomposition of primary ore minerals, metals and other potentially toxic elements are mobilized and then incorporated into secondary mineral phases. Some of these act as long-term sinks, effectively immobilizing (semi)metallic contaminants, while others serve as temporary reservoirs, releasing metals during changes in geochemical conditions prevailing in the weathering zone.

This study focuses on the Johan Hell mine, part of the Breiner deposit, which is notable for its Au-Ag mineralization, as well as for the presence of Zn, Pb, Cu, As and Sb. The primary objectives of this research were: to characterize the composition of secondary mineral assemblages in the various mine zones; and to evaluate the possible environmental impact of these phases.

* Corresponding author, e-mail: anna.januszewska@pgi.gov.pl

Received: June 26; accepted: November 13, 2025; first published online: December 9, 2025

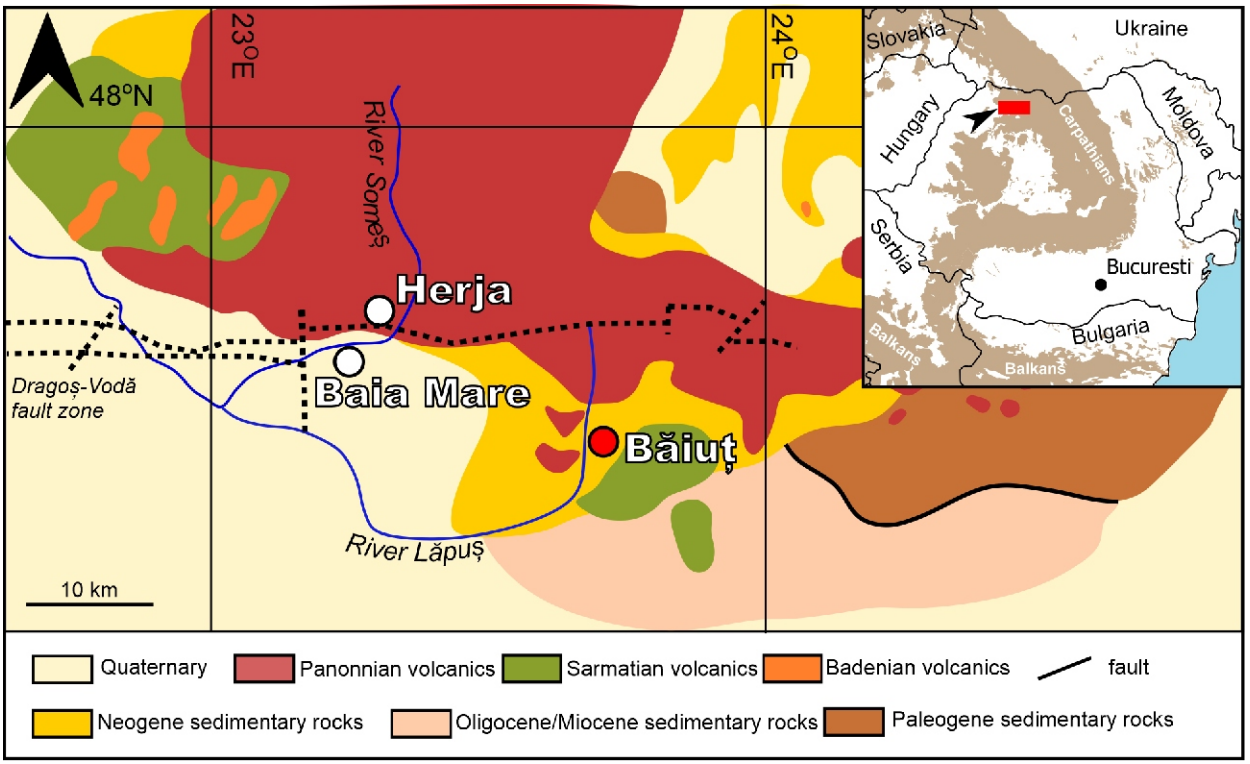

Fig. 1. Geological map of the Baia Mare area (after Kovács et al., 2009)

GEOLOGICAL SETTING

The Johan Hell mine is located in the Oaş-Gutâi Mountains, geologically situated within the Tocila-Secu Trans-Carpathian Flysch (Bombiță, 1972). Late Neogene porphyries intrude the sedimentary rocks in the area (Fig. 1). The evidence of volcanic activity observed in the region is attributed to a complex interplay of geological processes, including subduction, collision, and subsequent post-collisional and extensional events involving the southeastern border of the European and Alcapa-Tisia plates (Seghedi et al., 1998).The polymetallic deposits in the Baia Mare area are associated with the Dragoş Vodă fault zone (Fig.1, dotted lines) which is aligned E–W.

The deposits in the Baia Mare area are part of the Herja-Băiut metallogenic district, known for its Pb-Zn-Cu and Au-Ag mineralization (Kovacs and Fülöp, 2003). The ore mineralization in the broader Baia Mare region is classified as of low-sulphidation or adularia-sericite epithermal type (Grancea et al., 2002), associated with calc-alkaline volcanism (Iancu et al., 2010). However, recent studies conducted by Kovács and Tămaş (2020), on $Cu_3(As,Sb)S$ minerals from the Cisma and Herja mines, have revealed the presence of enargite and the luzonite-famatinite solid solution, typically associated with high-sulphidation deposits or occasional intermediate-sulphidation epithermal deposits.

The Breiner deposit encompasses a variety of Paleogene and Neogene sedimentary rock successions, primarily comprising marls, sandstones, and shales, with intrusions of Neogene andesite and diorite. The deposit in the vicinity of Băiuţ was exploited in two main mines: the Johan Hell mine (part of this study) and the Breiner mine. Within the sedimentary sequences, mineralized quartz veins, notably at Băiuț and Roba, intricately intersect, hosting a rich assortment of metallic minerals. Among the abundant ore minerals are pyrite, sphalerite, galena, chalcopyrite, marcasite, orpiment, realgar, arsenopyrite, pyrrhotite, stibnite, tetrahedrite group minerals (silver-enriched), native gold (*electrum*), and thioantimonate sulphosalts mainly represented by bournonite, jamesonite, and semseyite (Costin, 2000; Mariaş, 2005).

METHODOLOGY

Samples of weathering minerals were collected from one of the adits of the Johan Hell mine. Within the mining galleries surveyed, distinct zones containing weathering minerals were identified. The prominent area within this mine is a chamber with abundant forms of halotrichite group minerals. These minerals create structures resembling strands of hair, hanging from the walls of the mine, that can reach up to 1m in length (Fig. 2A), or create efflorescences on the mine walls (Fig.2B). Another noteworthy location is one of the old mine chambers where römerite-rich mineralization is present. These zones are located deep within the mine, ~3–4 km from the entrance. They are characterized by extremely dry conditions and a noticeable elevated temperature. Lastly, situated a little farther from the römerite-rich zone, is the voltaite-rich zone with abundant pyrite mineralization.

Samples of minerals from all the zones were collected and placed in airtight containers to prevent the loss of crystallization water. Phase composition analysis was conducted using the powder X-Ray diffraction method on an *X'Pert Pro* diffractometer at the Faculty of Geology, University of Warsaw, with the following parameters: current of 30 mA, voltage of 40 kV, and CoK anode *TOPAS* (v. 3.0) software with the Rietveld method were used for the qualitative phase analysis. For geochemical studies, 19 mineral samples (17 secondary minerals and 2 of pyrite ore) underwent chemical composition analysis using the ICP-MS/ES (*AQ250-EXT*) method at the Bureau Veritas laboratory in Canada. These analyses were carried out on mineral

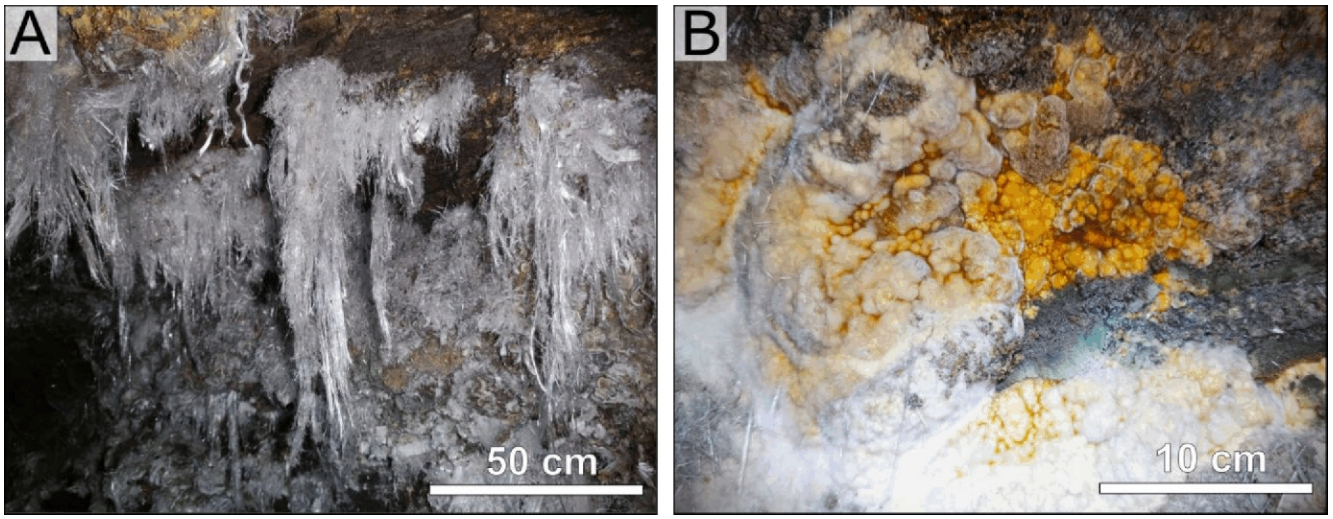

Fig. 2. Halotrichite group minerals in the Johan Hell mine

A – strains of hair-like crystals of halotrichite in the most prominent zone of the Johan Hell mine; **B** – cluster aggregates built with halotrichite group minerals

aggregates of typical composition. The sample mass depended on the mineral species. Römerite and voltaite were manually separated under a binocular microscope. Other minerals such as halotrichite gr., melanterite, hexahydrite and rozenite were selected as monomineral samples. Sample purity was verified microscopically and confirmed by X-ray diffraction. In cases where the material was not strictly monomineral, this was indicated as mineral parageneses (for example rozenite and hexahydrite). Overall, the specimens analysed are considered representative of the secondary sulphate assemblages studied.

Statistical analysis of the geochemical data was performed using principal component analysis (PCA) to identify underlying patterns and reduce data dimensionality. The analyses were carried out using *PAST* software version 4.13 (Hammer et al., 2001) and the RStudio environment.

RESULTS

SECONDARY MINERALS

In the Johan Hell mine, comprehensive survey has identified an assemblage of 20 distinct minerals or mineral groups. The most common are the **halotrichite-group minerals** (Figs. 2A,B, 3A, C, F, 4A and Table 1), which occur throughout all mine zones.

The halotrichite-group minerals are monoclinic, highly hydrated sulphates with the general formula $XY_2(SO_4)_4{\cdot}22H_2O$, where *X* is a divalent cation (commonly Fe^{2+}, Mg^{2+}, Mn^{2+}, Zn^{2+}, Co^{2+}) and *Y* is a trivalent cation (most commonly Al^{3+}, occasionally Fe^{3+} or Cr^{3+}; Ballirano, 2006). Crystallographically they belong to the space group $P2_1/c$, forming acicular (needle-like), fibrous or asbestiform aggregates, commonly as efflorescences, crusts or incrustations. Their crystal-chemical behaviour is dominated by extensive isomorphic substitution at the X-site among Fe^{2+}, Mg^{2+}, Mn^{2+} etc., and more limited substitution at the Y-site (Al^{3+} Fe^{3+}, Cr^{3+} in some samples; Ballirano, 2006).

Within this group, **halotrichite** is the most abundant in the Johan Hell mine and is particularly concentrated in a designated halotrichite gallery, where it forms notable, hair-like crystals that can exceed one metre in length and that are strikingly silver-white (Fig. 2A).

Additionally, **apjohnite** – the MnAl-dominant member of the halotrichite-group – was observed as efflorescent deposits on the mine walls, typically arranged in small circular clusters (Figs. 2B and 4A). While apjohnite generally presents a pristine white appearance, some specimens display a yellowish tint, likely resulting from jarosite encrustations.

In the mine, abundant magnesium sulphates were discovered, with **starkeyite** being the most common (Fig. 4B). This mineral is a member of the rozenite group which comprises hydrated sulphates with the general formula $MSO_4{\cdot}4H_2O$ (*M* = Mg^{2+}, Mn^{2+}, Fe^{2+}, Co^{2+}, Zn^{2+}, Cd^{2+}). Starkeyite coexisted with minerals of the halotrichite group, voltaite, szomolnokite, and other sulphates of divalent metals (rozenite, melanterite, epsomite, hexahydrite).

Hexahydrite occurs as white fibrous crystals on the mine walls, whereas starkeyite forms relatively hard, white to yellowish amorphous-like crusts. Additionally, minor amounts of sulphate minerals belonging to the epsomite group were identified via PXRD analysis in the samples containing halotrichite-group minerals, jarosite, starkeyite, and members of the rozenite group (Fig. 4A).

Jarosite, characterized by its finely crystalline yellow aggregates (Fig. 3A), was observed on the surface of barren rocks. Additionally, traces of this mineral were identified in samples containing copiapite and halotrichite-group minerals (Fig. 4C, D). In some cases, its presence may impart a yellowish colour to the minerals analysed.

Alunogen occasionally co-occurs with minerals from the halotrichite zone (Fig. 4C, D), forming spherical aggregates (Fig. 3B). Within these mineralized zones, copiapite – as the only representative of the copiapite group in the mine – is found in association with halotrichite, melanterite, rozenite, and fibroferrite (Fig. 4C). PXRD studies have also allowed detection of alum-(K) occurring alongside halotrichite-group minerals and jarosite. Additionally, simple zinc sulphates such as goslarite and bianchite are present in the mine, though they are relatively rare (Fig. 4A).

In the second prominent zone of the mine, rich **römerite**-bearing mineralization has been identified (Fig. 4D). The most characteristic component of this paragenesis is römerite This mineral forms euhedral crystals measuring up to a few millimetres in size, characterized by their distinctive brown-gold col-

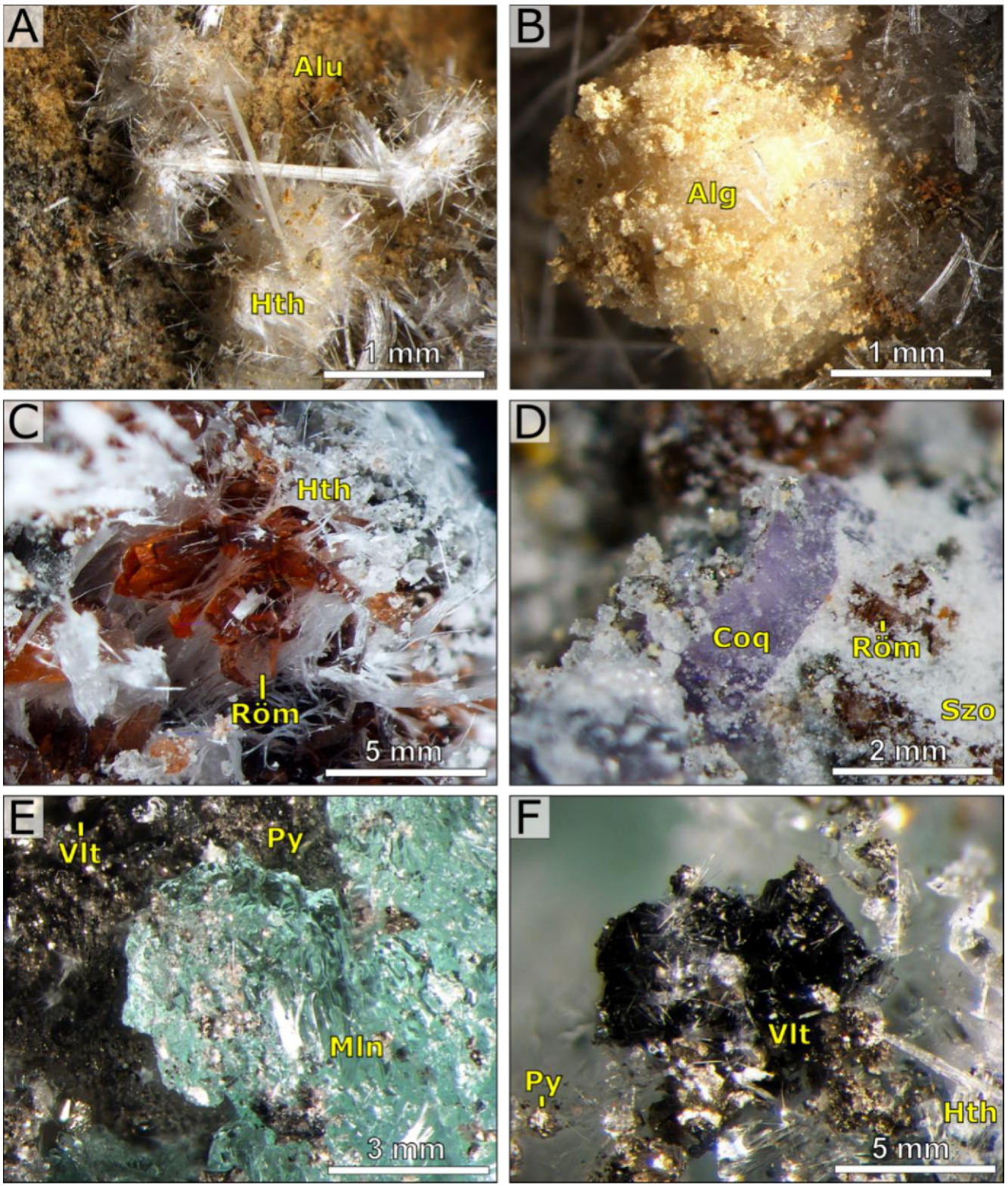

Fig. 3. Macro photos of minerals from the Johan Hell mine

A – halotrichite (Hth) euhedral crystals with small crystalline alunite group minerals (Alu); **B** – aggregate of alunogen (Alg); **C** – well-defined römerite (Röm) with halotrichite group minerals (Hth); **D** – coquimbite (Coq) with fine-grained szomolnokite (Szo) and small römerite (Röm) crystals; **E** – melanterite (Mlt) crust on pyrite (Py) with small crystals of voltaite (Vlt); **F** – voltaite euhedral crystal with hair-like halotrichite (Hth) and small crystal of pyrite (Py)

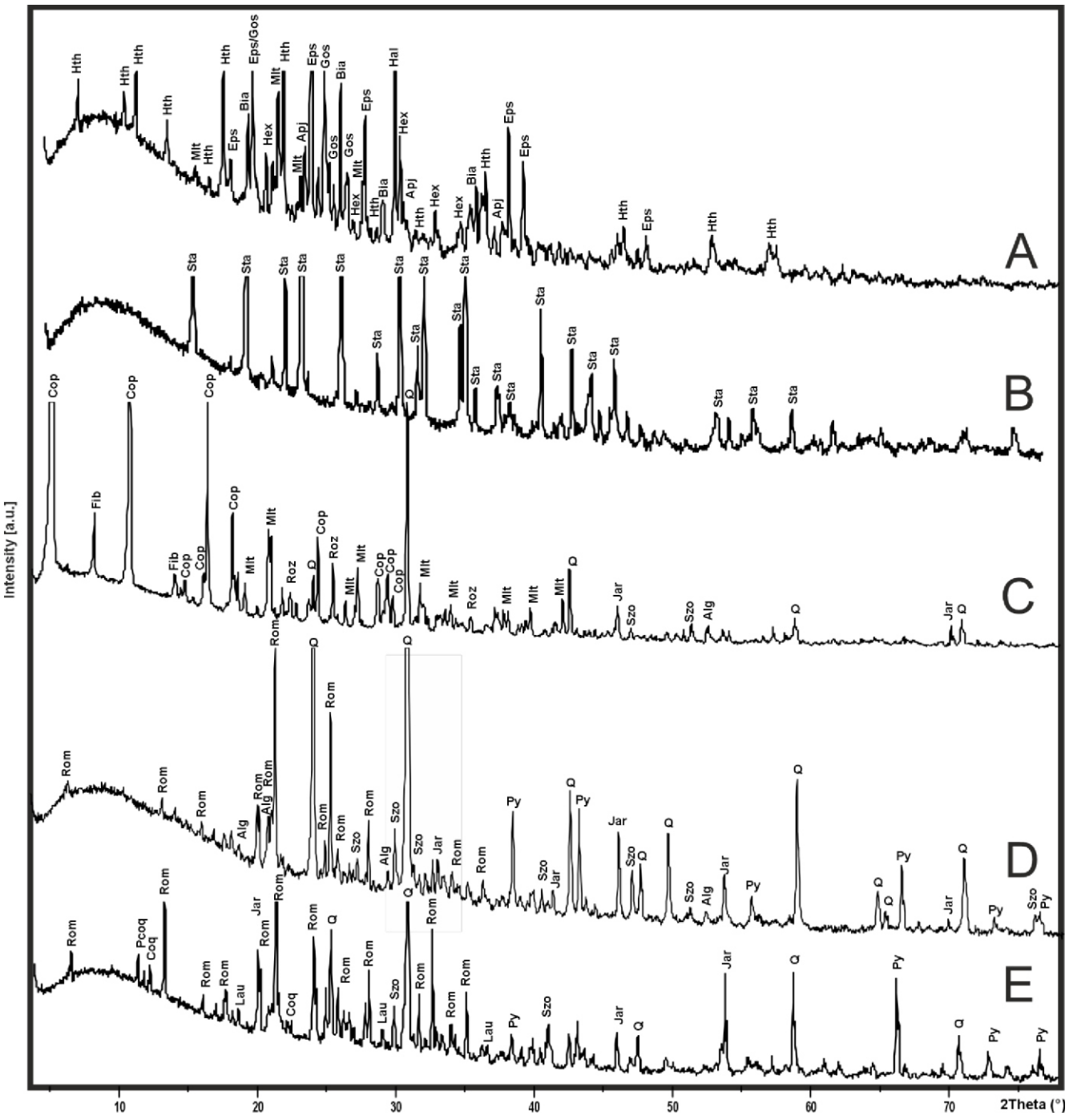

Fig. 4. PXRD patterns of secondary minerals from Johan Hell mine

Alg – alunogen, Apj – apjohnite, Bia – bianchite, Cop – copiapite, Coq – coquimbite, Eps – epsomite, Fib – fibroferrite, Gos – goslarite, Hth – halotrichite, Hex – hexahydrite, Jar – jarosite, Lau – lausenite, Mlt – melanterite, Pcoq – paracoquimbite, Py – pyrite, Q – quartz, Rom – römerite, Roz – rozenite, Sta – starkeyite, Szo – szomolnokite

our (Fig. 3C). Commonly, sugar-like crystals of szomolnokite are found coexisting alongside small, hair-like halotrichite (Figs. 4D and 5B). Light purple coquimbite crystals are also present within this paragenesis (Figs. 3D and 4E). Furthermore, rare secondary minerals were discovered through PXRD studies, including paracoquimbite and lausenite (Fig. 4E). These minerals were identified only sporadically, occurring in a single sample.

In the last distinctive zone, **voltaite** is the most characteristic mineral. This phase manifests as typical, black isometric crystals, forming directly on pyrite surfaces, together with melanterite, halotrichite and szomolnokite (Figs. 3E, F and 5A). The voltaite group consists of complex hydrated sulphates with the general formula $A_2Me2_5M1_3Al(SO_4)_{12}{\cdot}18H_2O$, crystallizing as black to dark-green octahedral or cubic crystals; they are characterized by high structural complexity and extensive isomorphic substitutions at the *Me* site (by Fe^{2+}, Mg^{2+}, Zn^{2+}, Mn^{2+}) and at the trivalent cation site *M1* (Al^{2+} Fe^{2+}, Cr^{2+}, V^{2+}). The *A* site of the mineral may be occupied by NH_4.

Szomolnokite in the mine occurs as sugar-like crystals, commonly associated with massive melanterite, fibrous halotrichite and euhedral voltaite (Fig. 4D, E). Voltaite crystals in the Johan Hell mine are small (up to 1–2 mm) and occasionally form intergrowths with melanterite. Similarly, halotrichite forms intergrowths with melanterite. Szomolnokite typically fills the spaces between these mineral phases.

Table 1

Secondary minerals identified in the Johan Hell mine with unit cell parameters data for selected minerals

Occurrence	Mineral	Chemical formula	Unit cell parameters						Statictic
			a [Å]	b [Å]	c [Å]	λ [°]	β [°]	γ [°]	
common	halotrichite	$FeAl_2(SO_4)_4{\cdot}22H_2O$	6.205(2)	24.330(45)	21.283(4)		100.29(2)		Rwp: 7.22%; GOF: 4.41%
common	apjohnite	$MnAl_2(SO_4)_4{\cdot}22H_2O$							
common	rozenite	$FeSO_4{\cdot}4H_2O$							
common	starkeyite	$MgSO_4{\cdot}4H_2O$							
common	melanterite	$Fe(H_2O)_6SO_4{\cdot}H_2O$	14.04(2)	6.520(7)	11.151(20)		106.20(15)		Rwp: 7.43%; GOF: 4.12%
common	hexahydrite	$MgSO_4{\cdot}6H_2O$							
common	epsomite	$MgSO_4{\cdot}7H_2O$	11.881(2)	12.037(2)	6.873(2)				Rwp: 7.22%; GOF: 4.41%
common	jarosite	$KFe_3(SO_4)_2(OH)_6$	7.342(1)		16.4(10)				Rwp: 7.22%; GOF: 4.41%
common	copiapite	$Fe^{2+}Fe^{3+}{}_4(SO_4)_6(OH)_2{\cdot}20H_2O$							
common	römerite	$Fe^{2+}Fe^{3+}{}_2(SO_4)_4{\cdot}14H_2O$							
common	voltaite	$K_2Fe^{2+}{}_5Fe^{3+}{}_3Al(SO_4)_{12}{\cdot}18H_2O$	27.261(16)						Rwp: 7.43%; GOF: 4.12%
common	coquimbite	$AlFe_3(SO_4)_6(H_2O)_{12}{\cdot}6H_2O$	10.944(14)		17.320(53)				Rwp: 9.17%; GOF: 5.16%
rare	bianchite	$ZnSO_4{\cdot}6H_2O$							
rare	goslarite	$ZnSO_4{\cdot}7H_2O$							
rare	alunogen	$Al_2(SO_4)_3{\cdot}17H_2O$	7.407(12)	27.200(37)	6.012(9)	89.95(10)	97.53(11)	91.77(13)	Rwp: 7.22%; GOF: 4.41%
rare	fibroferrite	$Fe^{3+}(SO_4)(OH){\cdot}5H_2O$							
very rare	szomolnokite	$FeSO_4{\cdot}H_2O$	7.029(10)	7.511(14)	7.817(8)		117.56(9)		Rwp: 9.17%; GOF: 5.16%
very rare	alum-(K)	$KAl(SO_4)_2{\cdot}12H_2O$							
very rare	paracoquimbite	$Fe_4(SO_4)_6(H_2O)_{12}{\cdot}6H_2O$	10.958(13)		51.660(76)				Rwp: 9.17%; GOF: 5.16%
very rare	lausenite	$Fe_2(SO_4)_3{\cdot}5H_2O$	10.776(14)	11.005(14)	5.630(8)		98.75(10)		Rwp: 9.17%; GOF: 5.16%

GEOCHEMICAL DATA

The geochemical composition of secondary minerals in the Johan Hell mine varies across different mineralization zones (Table 2). The trace-element composition of secondary sulphates from the halotrichite zone shows pronounced enrichment in several critical and toxic elements. Manganese is highly abundant (>10,000 ppm) in almost all phases, confirming its strong partitioning into hydrated Fe-sulphates such as halotrichite-group minerals, copiapite, melanterite, and rozenite. Zinc also reaches very high concentrations (>10,000 ppm) in several halotrichite-group samples, as well as in hexahydrite and rozenite.

Copper and lead are generally present in minor to moderate amounts (up to several hundred ppm), with occasional enrichments in halotrichite and jarosite samples (Pb 844 ppm) and copiapite (Pb 174 ppm). Notably, arsenic is markedly enriched in halotrichite and jarosite (up to 941 ppm) and copiapite (1187 ppm). Other trace metals such as Co, Ni and Cr are consistently present at tens to hundreds of ppm, confirming broad substitution at divalent cation sites. Highest Cr values was found in jarosite sample (Cr 501 ppm).

The rare earth elements measured (La+Y+Ce) are strongly variable, ranging from background levels to exceptionally high values in halotrichite-bearing assemblages (up to 1941 ppm). Elements such as Tl, Rb, Hg, Ag, and Au occur at very low concentrations (ppb–ppm range), though sporadic enrichments in Ag and Hg were detected (halotrichite-bearing samples, Ag up to 0.6 ppm; Hg up to 15.6 ppm).

Secondary sulphates from the römerite zone display a distinctive trace-element pattern compared with those from the halotrichite zone. Römerite itself shows low Mn contents (112 ppm), but is strongly enriched in Cu (2036 ppm), with some amounts of Pb (327 ppm), and Zn (2533 ppm). It also hosts exceptionally high concentrations of As (3736 ppm) and Sb (240 ppm). Precious metals are notably elevated, with Ag (38 ppm), Au (1.39 ppm), and Hg (16.6 ppm). Associated halotrichite-group minerals in this zone contain even higher Cu (7178 ppm) and significant enrichments in As (2052 ppm).

The voltaite zone is characterized by complex trace-element enrichments consistent with the structural flexibility of this mineral group. Voltaite itself contains moderate levels of Mn (443 ppm) but shows elevated Co (312 ppm) and As (2805 ppm). It also exhibits significant precious-metal contents (Ag 3.7 ppm, Au 2.6 ppm), and relatively high (in comparison to other secondary minerals) Rb and Tl, indicative of its capacity to accommodate large alkali ions within the structure. The associated halotrichite records elevated As (392 ppm) and Pb (113 ppm), together with measurable enrichments in Ag (0.88 ppm) and Au (0.23 ppm).

The pyrite ore samples (Table 3) are characterized by low Mn (~80 ppm) and Zn (80–135 ppm) compared with the extremely high contents in secondary sulphates (commonly >10,000 ppm). Copper and Sb are also distinctly lower in the ore (Cu <25 ppm; Sb <7.5 ppm) than in some secondary sulphates, where Cu commonly exceeds 2,000 ppm and Sb reaches 240 ppm in römerite.

Table 2

Geochemical composition of secondary mineral samples from the Johan Hell mine

Sample ID	Location	Identified minerals	Mn	Cu	Pb	Zn	Ni	Co	As	Cd	Cr	Sb	La+Y+Ce	Tl	Rb	Hg	Ag	Au
			ppm													ppb		
Jar	halotrichite zone	jarosite	>10000	21	29	5362	216	41	156	10	501	2.51	184	0.31	10	291	70	1.3
Cop		copiapite	4224	7.3	174	1964	46	8.6	1187	2.7	24	40.98	34	0.56	3.6	2524	193	3.7
Cop+Hth		copiapite, halotrichite gr.	>10000	61	11	3229	432	85	103	12	127	0.9	1007	0.11	3.1	656	45	0.6
Hth1		halotrichite gr.	1105	135	446	4405	22.3	36	40.7	22	44	0.28	1.9	0.2	0.5	64	523	5.3
Hth2		halotrichite gr.	>10000	3.4	14	>10000	319	30	49.7	25	13	1.54	111	<0.02	0.3	553	106	1
Hth3		halotrichite gr.	>10000	6.7	6.0	>10000	495	50	4.6	2.2	14	0.39	27	<0.02	0.2	81	24	<0.2
Hth+Jar1		halotrichite gr., jarosite	>10000	37	844	3234	530	121	724	12	164	34.54	1193	0.5	5.2	15571	639	12
Hth+Jar2		halotrichite gr., jarosite	>10000	7.1	24	3056	139	39	941	8.3	44	18.76	45	1.1	8	319	94	1.6
Hhy		hexahydrite	>10000	1.1	190	>10000	50.6	6.8	20.7	1.1	0.6	0.14	13.7	<0.02	0.3	99	94	<0.2
Mel		melanterite	>10000	0.44	1.6	3530	117	7.9	2.4	0.68	<0.5	0.62	8.5	<0.02	0.1	24	7	<0.2
Roz		rozenite	>10000	42	20	>10000	231	34	4.3	97	<0.5	1.13	3.1	<0.02	<0.1	48	45	0.5
Roz+Hhy		rozenite, hexahydrite	>10000	2.5	17	>10000	329	39	12.1	4.6	1.6	1.45	53	0.17	1.9	53	84	1.2
Str+Hth		starkeyite, halotrichite gr.	>10000	34	9	>10000	279	54	161	112	54	0.27	1941	0.03	0.4	47	79	1.5
Hth4	römerite zone	halotrichite gr.	217	7178	160	5277	37	50	2052	18	49	78.55	2.8	0.27	0.9	2403	2144	144
Röm		römerite	112	2036	327	2533	14	52	3736	6.1	14	240.67	6.2	0.45	1	38026	16633	1393
Hth5	voltaite zone	halotrichite	286	11	113	630	9.7	46	392	2.7	42	4.58	4.6	0.72	17	153	876	233
Vol		voltaite	443	46	221	1341	12	312	2805	5.3	3.9	12.83	9.9	6.79	95	366	3738	2595

Arsenic, however, is strongly enriched in both ore and secondary phases. The pyrite ore hosts As at 1300–1400 ppm, comparable to the range found in copiapite, but clearly lower than the extreme values in römerite (>3700 ppm) or voltaite (~2800 ppm). Cobalt is higher in the ore (190–249 ppm) than in most secondary sulphates, although voltaite again shows strong Co enrichment (312 ppm).

Pyrite ore is the primary host of Ag (6.2–8.8 ppm) and Au (1.1–1.4 ppm), which are concentrated also in römerite and voltaite. Mercury is elevated in pyrite (633–680 ppb), but secondary phases can locally reach even higher levels (e.g., römerite ~38,000 ppb). Pyrite ore represents the primary source of As, Co, Pb and precious metals (Ag, Au, Hg), subsequently mobilized and incorporated into secondary sulphates.

DISCUSSION

SECONDARY MINERALS FORMATION

The formation and stability of the secondary minerals in the Johan Hell mine are closely linked to changing environmental conditions. These factors have undergone significant shifts, primarily in terms of pH and humidity, influencing the crystallization, transformation and persistence of various mineral phases over time.

During the initial stage of mineral formation, the environment was characterized by extremely acidic conditions (pH <2) of pore solutions which were present in thin fissures that cut rocks bearing ore mineralization. Crystallization of these readily soluble sulphates as melanterite, epsomite and goslarite occurs in areas of exudation of acidic pore solutions on the walls of mine workings. Rapid evaporation of acidic pore solutions takes place at the elevated temperatures prevailing in the mine galleries studied (Fig. 6). At such temperatures, there is then a gradual loss of crystallization water from the precipitated sulphates and their slow transformation into phases with lower water contents. This shift led to the dehydration of the primary secondary minerals, forming rozenite, szomolnokite, hexahydrite, starkeyite and bianchite.

Another strong indicator of ultra-acidic conditions in this stage is the presence of alunogen, a sulphate mineral that forms as efflorescence from capillary solutions in extreme acidic environments (Nordstrom and Alpers, 1999). Additionally, minerals of the halotrichite group, which are most abundant, may have begun to crystallize during this phase. These minerals tend to form in highly acidic conditions and remain relatively stable despite humidity fluctuations (Hammarstrom et al., 2005; Sanchez, 2007).

The progressive oxidation of ferrous ions and the continued release of cations from the barren rock – driven by the aggressive action of sulfuric acid – marked the onset of the second major stage of mineral formation. With the gradual increase in pH (from ~1.2 to 3.0), mixed-valence and ferric sulphate minerals began to crystallize. This stage saw the formation of minerals such as lausenite, fibroferrite, copiapite, coquimbite and paracoquimbite. The subsequent formation of römerite indicates a further pH rise, as this mineral crystallizes from sulphate-rich solutions when Fe^{2+} partially oxidizes to Fe^{3+}, thereby reducing the overall acidity of the water (Frost et al., 2010; Murray et al., 2014).

Table 3

Geochemical composition of pyrite ore from the Johan Hell mine

Sample ID	Mn	Cu	Pb	Zn	Ni	Co	As	Cd	Cr	Sb	La+Y+Ce	Tl	Rb	Hg	Ag	Au
	ppm													ppb		
pyrite ore	82	24	964	80	3.5	249	1431	0.03	1.1	7.4	3.7	0.12	2.9	680	6248	1396
pyrite ore	77	18	1764	135	4.5	190	1304	0.07	1.1	5.5	4.2	0.13	3	633	8826	1081

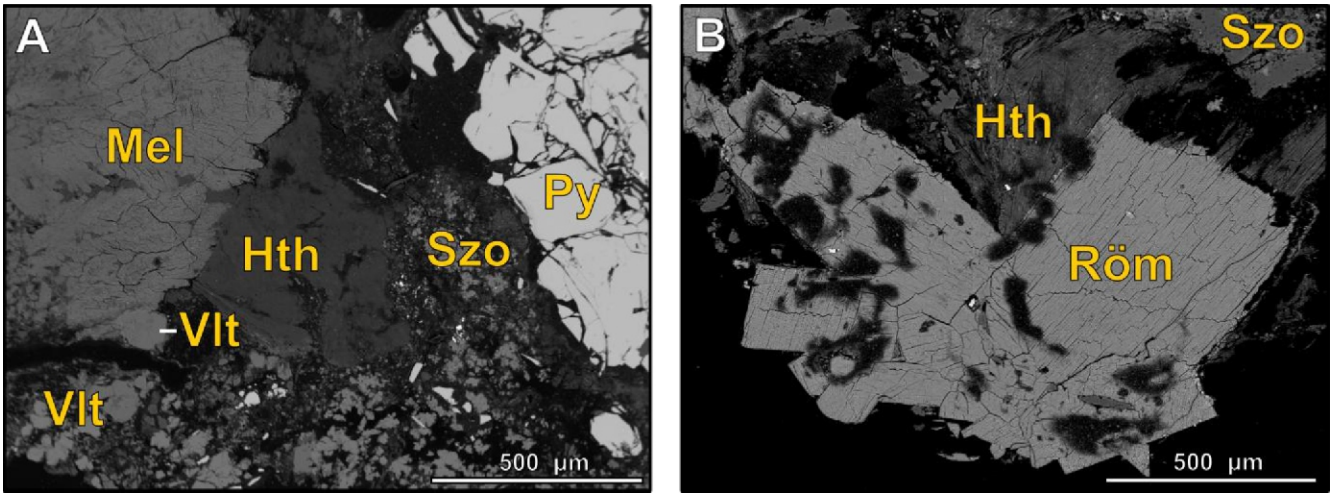

Fig. 5. Microphotographs taken using an electron microprobe of the sample containing voltaite (A) and the sample containing römerite (B)

A – paragenesis of compact melanterite (Mel) with halotrichite (Hth) intergrowths and voltaite (Vlt) inclusions, in contact with pyrite (Py). Intergranular spaces are filled with fragmented szomolnokite (Szo); **B** – Römerite (Röm) crystals associated with fibrous halotrichite (Hth) and szomolnokite (Szo)

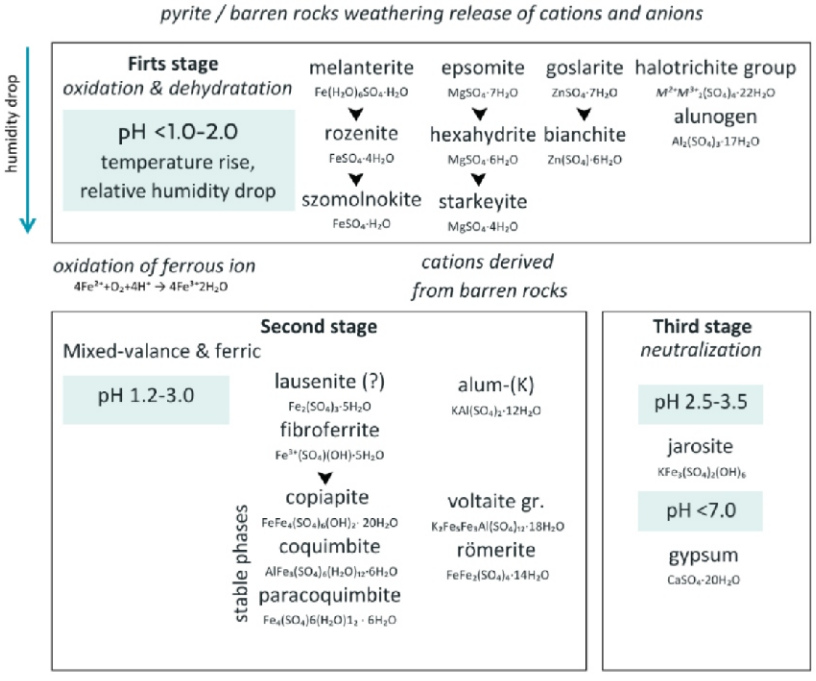

Fig. 6. Scheme of secondary mineral formation in Johan Hell mine

The continuous release of cations from barren rock (weathering of micas, K feldspars, and plagioclases) promoted the crystallization of voltaite, and alum-(K). The persistence of römerite and voltaite, which are commonly found within the mine, suggests that these conditions remained stable for an extended period.

In the final stage of secondary mineral formation, conditions within the mine stabilized at a higher pH range (2.5–3.5). This stage is characterized by the crystallization of jarosite, a mineral that typically forms in acidic aqueous solutions (Hammarstrom et al., 2005; Sanchez, 2007). A significant rise in pH facilitated the formation of more stable phases, such as gypsum, which are indicative of environments with reduced acidity.

Halotrichite group minerals are particularly abundant in the mine due to the prevailing dry environmental conditions, which prevent its dissolution and enhance its long-term stability. Its crystallization is closely linked to the presence of sulphuric acid, which is generated during the oxidation of sulphide minerals and plays a critical role in maintaining the extremely low pH necessary for halotrichite formation (Chou et al., 2013). Typically, this mineral forms in highly acidic settings, with pH values below 3.0, where the solubility of essential cations such as iron, magnesium, manganese and aluminium increases significantly, promoting their incorporation into the halotrichite structure (Sánchez et al., 2007). They can also form over a wider pH range, extending up to 3.5 (Stumbea et al., 2019).

The primary source of aluminium, a key component of this mineral group, is the breakdown of aluminosilicate minerals such as feldspars, and layered aluminosilicates. Furthermore, the hydration state of halotrichite underscores its dependence on water availability. It typically precipitates in low-temperature and high-humidity conditions, where sufficient water molecules integrate into its crystal lattice. Alpers et al. (1994) demonstrated through experimental studies that the halotrichite group forms from aqueous solutions at temperatures below 50°C. However, halotrichite can also develop in arid and semi-arid regions through the evaporation of sulphate-rich waters, demonstrating that its formation is not strictly limited to humid conditions.

COMPARISON WITH THE BREINER MINE

The Johan Hell mine is part of the larger Breiner deposit, which also includes the Breiner mine located beneath it. Despite their close proximity, the environmental conditions in these two mines differ significantly. While part of the Johan Hell mine is characterized by a warm and slightly humid environment, the Breiner mine is much colder and wetter. This contrast strongly influences the formation and stability of secondary minerals within each mine. In the Breiner mine, melanterite is the dominant secondary mineral (Januszewska et al., 2025), stabilized by persistently high-humidity conditions that prevent its transformation into lower-hydration sulphate phases. Although halotrichite-group minerals are also present, only species such as halotrichite and bílinite have been identified. Instead of forming as massive or large crystalline aggregates, they occur rather as small spherical aggregates on the surface of melanterite and along the mine walls. This suggests that their formation is influenced by local microenvironmental conditions, influenced by fluctuations in humidity and minor variations in pH, which may affect their crystallization pathways and stability within the Breiner mine.

A comparison of these two mines, both part of the same ore deposit, highlights the critical role of changing environmental conditions (such as pH, humidity) in influencing the composition of the secondary minerals. Efficient meteoric water supply in the Breiner mine enabled the formation of supersaturated solutions that persisted in the environment for an extended period, allowing melanterite crystallisation to dominate the secondary minerals in this part of deposit (Januszewska et al., 2025). By contrast, in the Johan Hell mine, the formation of supersaturated solutions was restricted, and ambient humidity levels favoured the persistence of halotrichite-group minerals. Melanterite occurs only locally, restricted to microenvironments with an increased influx of acid solutions. The assemblage of Fe-sulphate hydrates is predominantly composed of dehydrated phases such as rozenite and szomolnokite. This clear distinction underscores the importance of local humid conditions in controlling secondary mineral diversity and stability within mine settings.

MIGRATION OF ELEMENTS

Principal Component Analysis (PCA) was applied in this study as an exploratory multivariate method to identify associations between trace elements and the mineral groups. All datasets were normalized and centred prior to analysis to account for differences in chemical composition among diverse mineral species. PCA has been successfully applied in similar contexts, such as weathering zones and mine wastes, to reveal geochemical correlations (e.g., Foster et al., 2011; Byrne et al., 2017).

The minerals from the Johan Hell mine show significant variability in elemental distribution among secondary mineral species. The most compositionally diverse group comprises halotrichite-group minerals, which are also the most abundant and widely distributed in the part of the mine investigated. These minerals act as major sinks for a broad range of elements. PCA reveals that these samples are dispersed across different regions of the plot, indicating considerable compositional heterogeneity within this mineral group (Fig. 7).

For example, in zones where römerite is abundant, halotrichite-group minerals are more likely to incorporate elements that dominate in that specific geochemical environment, such as Cu, Pb, As, Hg, Au and Ag. Enrichment in elements such as Zn, Cu, Pb, Co and Cd is also observed in the halotrichite-group minerals. Compared to the Upper Continental Crust (UCC) standard (Fig. 8; Rudnick and Gao, 2003), the halotrichite group shows particularly high enrichment factors for Zn, As and Cd, reaching levels several hundred times greater than typical crustal values.

Halotrichite-group minerals are observed to sequester REE, locally exceeding 1000 ppm. A similar substitution mechanism has been documented at the sister Breiner mine (Januszewska et al., 2025) and in the Iberian Pyrite Belt (Soyol-Erdene et al., 2018). Compared to PAAS (Post-Archean Australian Shale; McLennan, 1989) these secondary minerals show REE concentrations that are several times higher. REEs show a strong correlation with Mn; this can be interpreted as a process signal of co-transport and partitioning into the same secondary phases. Although direct, mineral-specific datasets on REEs in halotrichite are scarce, studies of AMD systems shows that secondary sulphates (including halotrichite-group minerals within their assemblages) act as transient REE sinks via adsorption and coprecipitation, controlling REE fractionation and mobility in acidic environments (Fernández-Caliani, 2021; Soyol-Erdene et al., 2018; Gomes et al., 2022).

Voltaite is primarily enriched in elements directly inherited from the weathering of ore veins, mainly pyrite. These include Pb, As, Au, Ag, Tl, Co and Rb. The last three elements show relatively low diversity among secondary minerals, with their concentrations remaining fairly consistent (Fig. 8). By contrast,

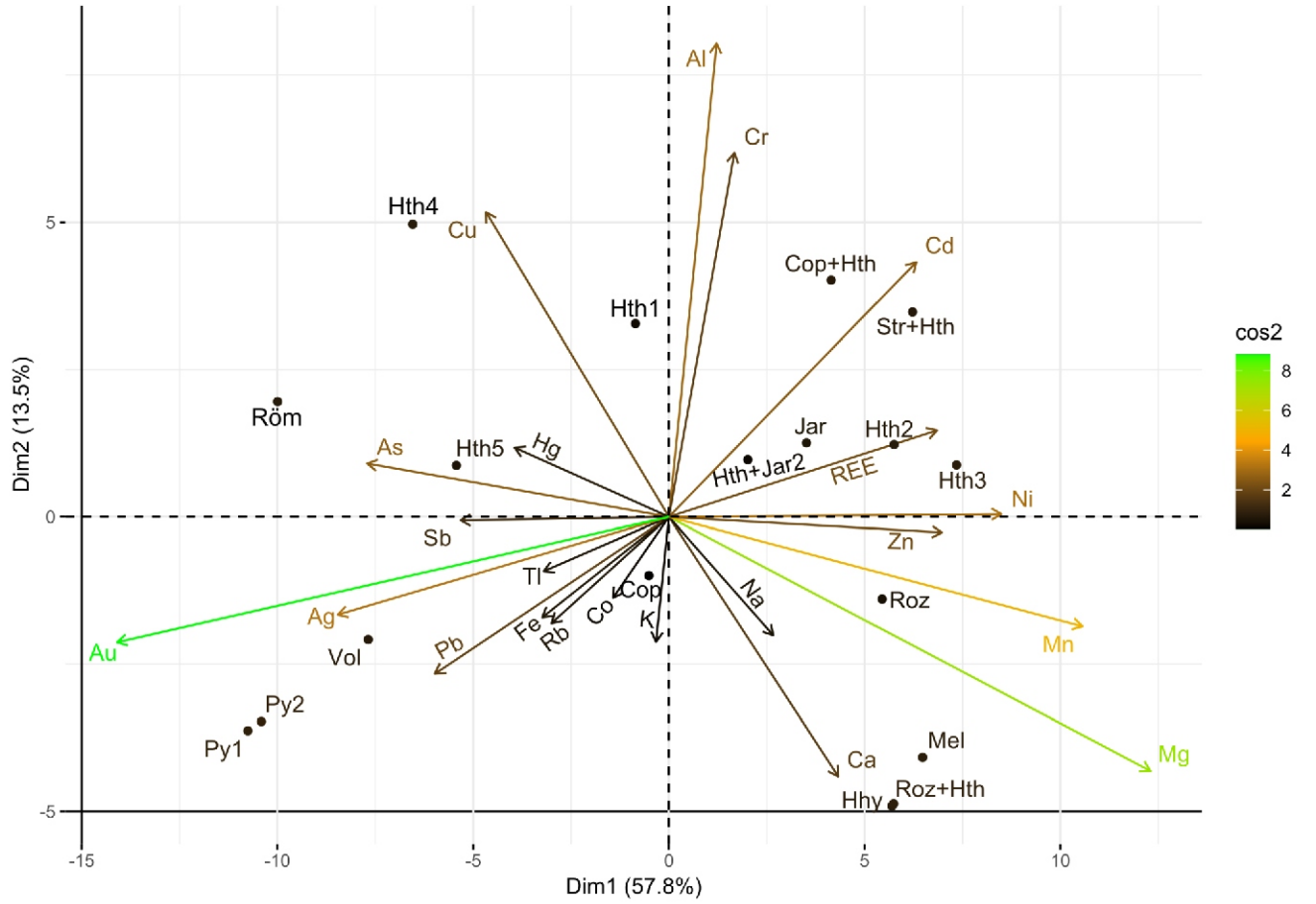

Fig. 7. PCA analysis of element distribution in the Johan Hell mine

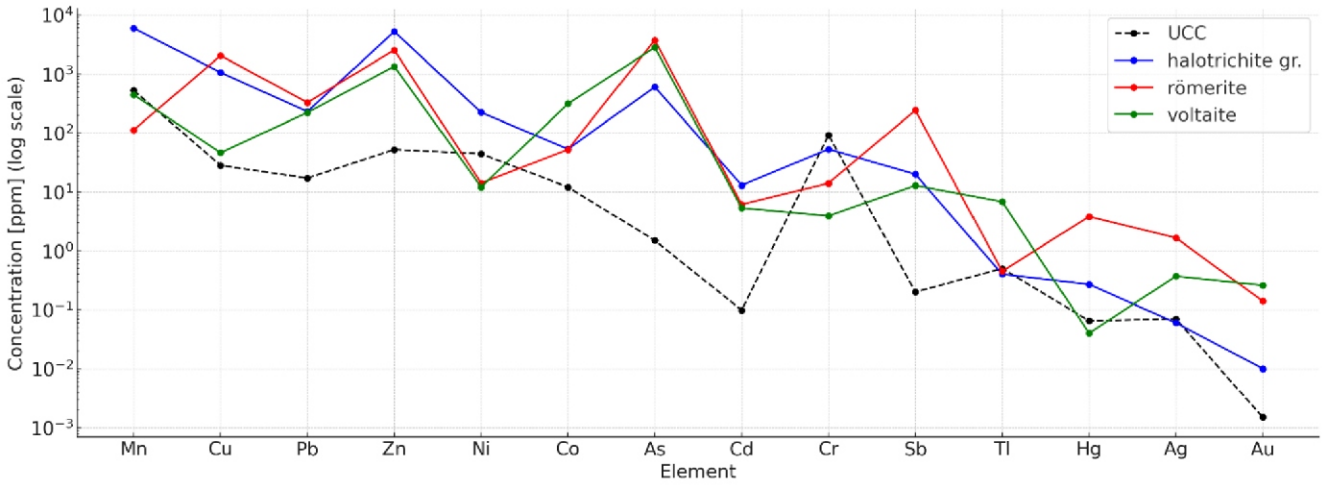

Fig. 8. Trace element concentrations in the most common secondary sulphate minerals from the Johan Hell mine in relation to Upper Continental Crust (UCC; Rudnick and Gao, 2003)

gold, followed by silver, shows the highest variability in mineralogical occurrence, displaying significant differences in concentration across various secondary mineral species. In the case of voltaite, compared to the UCC reference values (Fig. 8), gold shows the highest enrichment factor among all the mineral phases examined.

The calcium content in voltaite was significantly higher than that reported in earlier studies conducted on specimens from the Chiprovtsi ore field in Bulgaria (e.g., Dimitrova et al., 2019). Minerals of the voltaite group have a tendency to incorporate arsenic, which was previously reported in studies by Dimitrova et al. (2019), with concentrations ranging from 1,000 to more than 2,000 ppm. This exceeds the standard UCC values approximately a thousandfold (Fig. 8). Additionally, silver enrichment in this mineral was not consistently reported in previous research (Dimitrova et al., 2019).

Thallium is often known to be incorporated into the structure of voltaite (Biagioni et al., 2020b); however, this was not the case for samples from the Johan Hell mine. The ICP-MS results revealed that the highest concentrations of thallium were indeed found in voltaite, though reaching only up to 6.8 ppm. Other element substitutions within the mineral structure, such as Mg, Mn, or Al, have been previously reported (Biagioni et al., 2020a; Zhitova et al., 2023).

Römerite displays a distinct geochemical composition in comparison to the other minerals, occupying the opposite end of the PCA plot alongside minerals that share a paragenetic association with it (Fig. 7). Both römerite and halotrichite from the römerite-rich zone show the highest arsenic concentrations, likely resulting from the enrichment of the ore minerals in this element. Additionally, arsenic shows a positive correlation with Au, Ag and Hg, and this enrichment is similarly evident in römerite. Arsenic uptake in römerite was previously reported by Dimitrova et al. (2019), with values ranging between 400 and 500 ppm. By contrast, samples from the Johan Hell mine show arsenic incorporation several orders of magnitude higher (As >3700 ppm).In relation to UCC, römerite displays the highest enrichment factor of As (Fig. 8). Silver and mercury substitution is uncommon for this type of mineral, as it has not been reported at such levels in previous research. Conversely, copper enrichment in this phase has also been documented in samples collected from the Chiprovtsi ore field in Bulgaria (Dimitrova et al., 2019). Römerite can accommodate various cations at the *A* site of its crystal structure. For example, samples from the Apuan Alps show substitution by Mg (Mauro et al., 2018). In the case of the Johan Hell mine, we observed the incorporation of Zn, and to some extent Na. This substitution is related to the availability of Zn ions in the system, which results from the oxidation of polymetallic mineralization rich in sphalerite.

Hydrated divalent cation sulphates, such as melanterite, rozenite, epsomite and hexahydrite, show similar trace element compositions. These minerals are closely positioned on the PCA plot and are predominantly composed of Ca, Mg, Na and Mn. Substitution of these elements is most commonly observed within this group of minerals. However, the diversity of Mg and Mn across the secondary minerals varies significantly. Zinc and nickel exhibit a linear correlation, suggesting similar geochemical behaviour and substitution within the mineral structures (e.g., in melanterite and rozenite). By contrast, the antimony vector is inversely correlated with Zn and Ni. This element is primarily concentrated in different minerals, such as those associated with the halotrichite group, as well as jarosite, copiapite and römerite.

When considering the origin of metals incorporated into secondary sulphates, it is important to note that they do not derive solely from the oxidation of sulphide ores. Their composition also reflects the breakdown of barren host minerals under acidic conditions. Elements such as Mg and Fe can be released from chlorite, amphiboles and pyroxenes; Al from aluminosilicates including feldspars, muscovite, illite and kaolinite; and K and Na from feldspars and micas. Manganese may originate from Mn-carbonates, while Ca can be supplied by plagioclase. As a result, the chemistry of secondary sulphates records contributions both from the alteration of ore sulphides and from the parallel decomposition of easily weathered gangue minerals. In addition, pyrite ore represents the main source of As, Co and Pb, as well as precious metals such as Ag, Au and Hg, which are mobilized during weathering and subsequently incorporated into secondary sulphate phases.

From an environmental perspective, the ability, e.g., of halotrichite-group minerals, römerite and voltaite to incorporate and only temporarily immobilize toxic elements such as As, Cu, Zn, Cd, Pb and Hg is of particular concern. Because these secondary sulphates are highly soluble and unstable under changing humidity or pH conditions, their dissolution can rapidly release contaminants into surface and groundwater. Such processes are known drivers of severe acid mine drainage impacts worldwide, for example in the Iberian Pyrite Belt (Spain), where the long-term weathering of massive sulphide deposits has created highly acidic rivers enriched in Fe, As and heavy metals, and in the Berkeley Pit, Butte, Montana (USA), where AMD has generated a toxic lake containing extremely high metal concentrations. In the Breiner–Băiuţ mining area (Romania), weathering zones with efflorescent secondary sulphates exert a strong negative impact on local waters by contributing to acid mine drainage and releasing Cu, Zn, Fe and other toxic elements into adjacent streams at concentrations far exceeding environmental thresholds (Iepure et al., 2025). These examples highlight that the instability of secondary sulphates can transform mining wastes into a persistent source of metal contamination in surface waters.

CONCLUSION

This study investigated the secondary sulphate mineral assemblages formed under active weathering conditions in the Johan Hell mine, located in the Baia Mare metallogenic district of northern Romania. The mine, part of the Breiner deposit, is characterized by Au-Ag polymetallic mineralization and intense supergene alteration. Detailed mineralogical and geochemical (ICP-MS/ES) analyses allowed the identification of 20 secondary sulphate phases, dominated by halotrichite-group minerals, römerite, voltaite, melanterite, starkeyite, hexahydrite, epsomite, rozenite, szomolnokite and copiapite.

The mineral assemblages reflect a multi-stage formation history controlled by variable pH and moisture conditions. Early-forming phases such as melanterite and epsomite are associated with extreme acidity and high humidity, while dehydrated sulphates and mixed-valence minerals (e.g., römerite, voltaite) indicate subsequent shifts in environmental parameters. The Johan Hell mine's dry and warm microclimate favored the preservation of low-hydration minerals, in contrast to the adjacent Breiner mine, where high humidity supports melanterite stability.

The geochemical composition of the secondary minerals highlights their role as sinks for toxic and critical elements, including Fe, As, Sb, Cu, Pb, Zn, Hg and REEs. Particularly, halotrichite and römerite show exceptional enrichment in arsenic and trace metals, suggesting potential environmental risk. Principal Component Analysis (PCA) corroborated the compositional heterogeneity and mineral-specific elemental associations.

The findings contribute to a better understanding of sulphate mineral evolution in ore weathering environments and underline the importance of local climatic and geochemical controls on secondary mineral paragenesis. This knowledge is essential for assessing environmental impacts and potential remediation strategies in post-mining landscapes.

Acknowledgements. The authors gratefully acknowledge the financial support provided in part by the grant no. BOB-IDUB-622-330/2025, awarded within the framework of the "Excellence Initiative – Research University" programme at the University of Warsaw. This funding significantly contributed to the successful completion of the research presented in this article.

REFERENCES

Alpers, C.N., Blowes, D.W., Nordstrom, D.K., Jambor, J.L., 1994. Secondary minerals and acid mine-water chemistry. In: The Environmental Geochemistry of Sulfide Mine-wastes, Chapter **9** (eds. J.L. Jambor and D.W. Blowes): 246–270. Mineralogical Association of Canada.

Ballirano, P., 2006. Crystal chemistry of the halotrichite group $XAl_2(SO_4)_4{\cdot}22H_2O$: the X= Fe-Mg-Mn-Zn compositional tetrahedron. European Journal of Mineralogy, **18**: 463–469; https://doi.org//10.1127/0935-1221/2006/0018-0463

Biagioni, C., Mauro, D., Pasero, M., 2020a. Sulphates from the pyrite ore deposits of the Apuan Alps (Tuscany, Italy): a review. Minerals, **10**, 1092; https://doi.org/10.3390/min10121092

Biagioni, C., Mauro, D., Pasero, M., Bonaccorsi, E., Lepore, G.O., Zaccarini, F., Skogby, H., 2020b. Crystal-chemistry of sulphates from the Apuan Alps (Tuscany, Italy). VI. Tl-bearing alum-(K) and voltaite from the Fornovolasco mining complex. American Mineralogist, **105**: 1088–1098; https://doi.org/10.2138/am-2020-7320

Bombiță, G., 1972. Lăpuş Mountains geological research (in Romanian). Anuarul Institutului Geologic al României, **39**: 7–100.

Byrne, P., Wood, P.J., Reid, I., 2017. The use of synoptic sampling and multivariate statistical analysis to identify sources of metals in streams affected by acid mine drainage. Environmental Science and Pollution Research, **24**: 17220–17240; https://doi.org/10.1007/s11356-017-9038-x

Chou, I.M., Seal, R.R.I., Wang, A., 2013. The stability of sulphate and hydrated sulphate minerals near ambient conditions and their significance in environmental and planetary sciences. Journal of Asian Earth Sciences, **62:** 734–758; https://doi.org/10.1016/j.jseaes.2012.11.027

Costin, D., 2000. Major Elements Geochemistry of the Breiner Baiut Ore Deposit (Gutai Mountains, Eastern Carpathians). Studia UBB Geologia, **45:** 55–66.

Costin, D., 2003. Compositional data on boumonite-$CuPbSbS_3$ from Varatec ore deposit, Baiut mine field, Eastern Carpathians, Romania. Studia UBB Geologia, **48**: 45–54.

Costin, D., Vlad, S., 2005. Ore formation at Varatec-Baiut, Baia Mare region, East Carpathians, Romania. Geochemistry, Mineralogy and Petrology (Sofia), **43:** 64–68.

Damian, G., Ciobanu, C.L., Cook, N.J., Damian, F., 2008. Bismuth sulphosalts from the galena-matildite series in the Cremenea vein, Şuior, Baia Mare district, Romania. Neues Jahrbuch für Mineralogie Abhandlungen, **185**: 199–213; https://doi.org/10.1127/0077-7757/2008/0118

Damian, G., Buzatu, A., Apopei, I.A., Szakács, Z.L., Denuţ, I., Iepure, G., Bârgăoanu, D., 2020. Valentinite and colloform sphalerite in epithermal deposits from Baia Mare Area, Eastern Carpathians. Minerals, **10**, 121; https://doi.org/10.3390/min10020121

Dimitrova, D., Mladenova, V., Hecht, L.,2019. Efflorescent sulphate crystallization on fractured and polished colloform pyrite surfaces: A migration pathway of trace elements. Minerals, **10**, 12; https://doi.org/10.3390/min10010012

Dorotan, D., Costin, D., Ozunu, A., 2018. Application of quality indices for evaluation of heavy metals pollution in water, soil and sediments in the Upper Lapus River, Baiut mining district, Maramures County, Romania. Journal of Environmental Protection and Ecology, **19:** 1472–1480.

Fernández-Caliani, J.C., Grantcharova, M.M., 2021. Enrichment and fractionation of rare earth elements in an estuarine marsh soil receiving acid discharges from legacy sulfide mine wastes. Soil Systems, **5**, 66; https://doi.org/10.3390/soilsystems5040066

Foster, A.L., Brown, G.E., Tingle, T.N., Parks, G.A., 2011. Quantitative arsenic speciation in mine wastes and natural soils by X-ray absorption spectroscopy. Geochemical Transactions, **12**, 1; https://doi.org/10.1186/1467-4866-12-1

Frentiu, T., Ponta, M., Levei, E., Gheorghiu, E., Benea, M., Cordos, E., 2008. Preliminary study on heavy metals contamination of soil using solid phase speciation and the influence on groundwater in Bozanta–Baia Mare Area, Romania. Chemical Speciation and Bioavailability, **20:** 99–109; https://doi.org/10.3184/095422908X324471

Gomes, P., Valente, T., Marques, R., Prudęncio, M.I., Pamplona, J., 2022. Rare earth elements-source and evolution in an aquatic system dominated by mine-influenced waters. Journal of Environmental Management, **322**, 116125; https://doi.org/10.1016/j.jenvman.2022.116125

Grancea, L., Bailly, L., Leroy, J., Banks, D., Marcoux, E., Milési, J., Cuney, M., André, A., Istvan, D., Fabre, C., 2002. Fluid evolution in the Baia Mare epithermal gold/polymetallic district, Inner Carpathians, Romania. Mineralium Deposita, **37:** 630–647; https://doi.org/10.1007/s00126-002-0276-5

Hammarstrom, J.M., Seal, I.R.R., Meier, A.L., Kornfeld, J.M., 2005. Secondary sulphate minerals associated with acid drainage in the eastern US: recycling of metals and acidity in surficial environments. Chemical Geology, **215:** 407–431; https://doi.org/10.1016/j.chemgeo.2004.06.053

Hammer Harper, D.A.T., Ryan, P.D., 2001. PAST: Paleontological Statistic software package for education and data analysis. Palaeontologia Electronica, **4**, 9.

Iancu, O.G., Kovács, M., Fülöp, A., Balintoni, I., Constantinescu, E., Anastasiu, N., Răileanu, M., 2010. Ore deposits and other classic localities in the Eastern Carpathians: from metamorphics to volcanics. Acta Mineralogica-Petrographica, Field Guide Series, **19:** 1–55.

Iepure, S., Nagy, L., Momeu, L., Baciu, C., 2025. Treatment of acid mine water from the Breiner–Băiuţ area (Romania). Water, **17**, 225; https://doi.org/10.3390/w17020225

Januszewska, A., Siuda, R., Kruszewski, Ł., 2025. Composition and geochemistry of recently formed secondary mineral parageneses from the Breiner mine, Maramureş, Romania. Journal of Geochemical Exploration, **269**, 107638; https://doi.org/10.1016/j.gexplo.2024.107638

Kovács, M., Fülöp, A., 2003. Neogene volcanism in Gutâi Mts. (Eastern Carpathians): a review. Studia UBB Geologia, **48**: 3–16; httsp://doi.org/10.5038/1937-8602.48.1.1

Kovács, M., Fülöp, A., 2009. Baia Mare Geological and Mining Park – a potential new Geopark in the northwestern part of Romania. Studia UBB Geologia, **54:** 27–32; https://doi.org/10.5038/1937-8602.54.1.6

Kovács, R., Tămaş, C.G., 2020. $Cu_3(As,Sb)S_4$ minerals from the Baia Mare metallogenic district, Eastern Carpathians, Romania-a case study from the Cisma ore deposit. Geological Quarterly, **64** (2): 263–274; https://doi.org/10.7306/gq.1529

Lang, B., 1979. The base metals-gold hydrothermal ore deposits of Baia Mare, Romania. Economic Geology, **74:** 1336–1351; https://doi.org/10.2113/gsecongeo.74.6.1336

Lang, B., 1994. Ar-Ar dating of adularia – a tool in understanding genetic relations between volcanism and mineralization: Baia Mare area (Gutai Mountains), northwestern Romania. Economic Geology, **89**: 174–180; https://doi.org/10.2113/gsecongeo.89.1.174

Levei, E., Frentiu, T., Ponta, M., Senila, M., Miclean, M., Roman, C., Cordos, E., 2009. Characterisation of soil quality and mobility of Cd, Cu, Pb, and Zn in the Baia Mare area Northwest Romania following the historical pollution. International Journal of Environmental and Analytical Chemistry, **89:** 635–649; https://doi.org/10.1080/03067310902792586

Mariaş, Z.F., 2005. Metallogeny of the Baia Mare mining district. An approach based on the Cavnic hydrothermal system, comparison with other epithermal systems in the world (in Romanian): 378–450. Cornelius Publishing House.

Mauro, D., Biagioni, C., Pasero, M., 2018. Crystal-chemistry of sulphates from Apuan Alps (Tuscany, Italy). I. Crystal structure and hydrogen bond system of melanterite, $Fe(H_2O)_6(SO_4)\cdot H_2O$. Periodico di Mineralogia, **87:** 85–92; https://doi.org/10.2451/2018PM759

McLennan, S.M., 1989. Rare Earth Elements in sedimentary rocks: Influence of Provenance and Sedimentary Process. Review of Mineralogy, **21:** 169–200; https://doi.org/10.1515/9781501509032-010

Murray, J., Kirschbaum, A., Dold, B., Guimaraes, E., Miner, E., 2014. Jarosite *versus* soluble iron-sulphate formation and their role in acid mine drainage formation at the Pan de Azúcar Mine tailings (Zn-Pb-Ag), NW Argentina. Minerals, **4**: 477–502; https://doi.org/10.3390/min4020477

Nordstrom, D.K., Alpers, C.N., 1999. Negative pH, efflorescent mineralogy, and consequences for environmental restoration at the Iron Mountain Superfund site, California. Proceedings of the National Academy of Sciences, **96:** 3455–3462; https://doi.org/10.1073/pnas.96.7.3455

Plotinskaja, O., Damian, F., Prokofiew, W., Kowalenker, W., Damian, G., 2009. Tellurides occurrences in the Baia Mare region, Romania. Carpathian Journal of Earth and Environmental Sciences, **4:** 89–100.

Popa, G., Mihaiescu, T., Odagiu, A., Mihaiescu, R., Balint, C., Oltean, I., 2019. Heavy metals accumulation in riparian vegetation in Baiut metallogenic area, Maramures county (Romania). CHEMIA, **2**, 457; https://doi.org/10.24193/subbchem.2019.2.39

Rudnick, R.L., Gao, S., 2003. Composition of the continental crust. Treatise on Geochemistry, **3:** 1–64; https://doi.org/10.1016/B0-08-043751-6/03016-4

Sánchez, E.J., Santofimia, P.E., López, P.E., 2007. Iron terraces in acid mine drainage systems: a discussion about the organic and inorganic factors involved in their formation through observations from the Tintillo acidic river (Riotinto mine, Huelva, Spain). Geosphere, **3:** 133–151; https://doi.org/10.1130/GES00069.1

Santanna, D., Aryampa, A., Jordan, G., Gheorghe, D., Szabo, C., 2021. Geochemical characteristics and water pollution by Potentially Toxic Elements at the Văratec creek, Băiuţ mining area, Romania. In EGU General Assembly Conference Abstracts, EGU21-13995; https://doi.org/10.5194/egusphere-egu21-13995

Seghedi, I., Balintoni, I., Szakács, A., 1998. Interplay of tectonics and Neogene post-collisional magmatism in the Intracarpathian region. Lithos, **45:** 483–497; https://doi.org/10.1016/S0024-4937(98)00046-2

Soyol-Erdene, T.O., Valente, T., Grande, J.A., de la Torre, M., L., 2018. Mineralogical controls on mobility of rare earth elements in acid mine drainage environments. Chemosphere, **205:** 317–327; https://doi.org/10.1016/j.chemosphere.2018.04.095

Stumbea, D., Chicoş, M.M., Nica, V., 2019. Effects of waste deposit geometry on the mineralogical and geochemical composition of mine tailings. Journal of Hazardous Materials, **368:** 496–505; https://doi.org/10.1016/j.jhazmat.2019.01.071

Warr, L.N., 2021. IMA–CNMNC approved mineral symbols. Mineralogical Magazine, **85**: 291–320; https://doi.org/10.1180/mgm.2021.43

Zhitova, E.S., Sheveleva, R.M., Kupchinenko, A.N., Zolotarev, A.A., Pekov, I.V., Nuzhdaev, A.A., Semenova, T.F., 2023. The crystal chemistry of Voltaite-group minerals from post-volcanic and anthropogenic occurrences. Symmetry, **15**, 2126; https://doi.org/10.3390/sym15122126